Arabian Journal of Chemistry (2023) **16**, 105124

King Saud University

Arabian Journal of Chemistry

www.ksu.edu.sa
www.sciencedirect.com

ORIGINAL ARTICLE

Cu-decorating on N, P-Codoped porous carbon derived from wheat straw as advanced catalysts for N-alkylation of amines with alcohols

Dong Zhang [a], Jingjing Tian [a], Yunyun Yan [a], Lina Zhang [a,*], Hongyu Hu [b,*]

[a] *Shaanxi Key Laboratory of Phytochemistry and College of Chemistry and Chemical Engineering, Baoji University of Arts and Sciences, Baoji 721013, China*
[b] *Xingzhi College, Zhejiang Normal University, Lanxi 321004,China*

Received 3 April 2023; accepted 29 June 2023
Available online 3 July 2023

KEYWORDS

N, P-Codoped porous carbon;
Biomass resources;
Cu-based catalysts;
N-alkylation;
Alcohol

Abstract The design and fabrication of highly efficient, cheap, and stable heterogeneous catalyst for the advancement of sustainable organic transformation is a crucial goal in both academic research and industry. Herein, an efficient catalyst based on Cu-decorating on a N, P-codoped porous carbon(Cu/NPC) derived from wheat straw was successfully synthesized by a cost-effective method. The as-prepared Cu/NPC showed superior catalytic activity for the N-alkylation of amines with alcohols via the borrowing hydrogen strategy. A variety of aromatic amines were converted into the corresponding secondary amines in moderate to excellent yields. Noted that, such catalyst can be easily prepared, recovered and recycled four times without obvious loss in both activity and selectivity.

1. Introduction

N-alkyl amines and their derivations are an important class of chemicals utilized as building blocks for the generation of dyes, pharmaceuticals, agrochemicals, polymer and bioactive molecules (Carey et al., 2006; Chang and Chow, 2009; Froidevaux et al., 2016; Lengvinaite et al., 2008). Benefiting from their wide range of applications, the design and development of cost-effective and facile synthetic methods for N-alkylation of amines is highly desirable. Among numerous synthetic strategies (Veefkind and Lercher 1998, Hayes 2001, Martínez-Asencio et al., 2011), the N-alkylation of amines with alcohols is an efficient and sustainable approach, which follows the borrowing hydrogen or hydrogen auto-transfer. Generally, such hydrogen borrowing approach consists of three different steps: (i) the alcohol is catalyzed by a transition-metal catalyst to produce the corresponding carbonyl compound; (ii) the carbonyl compound is condensed with the amine to form the imine, and (iii) finally the imines is reduced to N-alkylamine by using the metal hydride produced in the alcohol dehydrogenation step (Guillena et al., 2010, Irrgang and Kempe 2019). It is should be noted that, in this transformation process, water is the only by-product as well as alcohol is also inexpensive as an alkylation reagent owing to its abundant supply from biomass degradation.

* Corresponding authors.
E-mail addresses: feimengxia_123@163.com (L. Zhang), huhongyu22@126.com (H. Hu).

Peer review under responsibility of King Saud University.

Production and hosting by Elsevier

https://doi.org/10.1016/j.arabjc.2023.105124
1878-5352 © 2023 The Author(s). Published by Elsevier B.V. on behalf of King Saud University.

Up to now, there are many homogeneous catalytic systems based on Ir (Jiménez et al., 2018, Huang et al., 2019, Li et al., 2019, Luo et al., 2020, Feng and Huang 2021), Ru (Huang et al., 2021, Karaca et al., 2021), Rh (Wong et al., 2017), Mn (Fertig et al., 2018, Wei et al., 2021), Ni (Vellakkaran et al., 2017, Balamurugan et al., 2020), Co (Rosler et al., 2015, Emayavaramban et al., 2019, Prabha et al., 2021), Fe (Minakawa et al., 2015), Cr (Kallmeier et al., 2020) complexes for the N-alkylation of amine with alcohol. However, the above-mentioned catalytic systems suffer from some drawbacks, including low catalyst reusability and the use of expensive ligands. Therefore, find out an efficient strategy to overcome the above drawbacks is very important. Recently, the construction of heterogeneous catalyst has proven an efficient route that can overcome these disadvantages of homogeneous catalyst. Hence, the development of efficient and highly selective heterogeneous catalysts for the N-alkylation of amine with alcohol is highly desirable. Until now, different types of heterogeneous catalysts have been designed for this transformation such as Au/TiO_2 (He et al., 2010), Pd/C (Liu et al., 2016), Pd/MgO (Corma et al., 2010), Pd/SiO_2 (Alshammari et al., 2020), $PdCeNi_XO_Y$ (Zhang et al., 2019), $PdZn/Al_2O_3$ (Furukawa et al., 2016), $Fe_{10}Pd_1$/NC500 (Wu et al., 2021), Ag@polypyrrole material (Mandi et al., 2016), Ag/Mo (Cui et al., 2011), $Ag@Al_2O_3$ (Paul et al., 2017), Co_2Rh_2/C (Chung and Chung 2018), Ni/Al_2O_3 (Shimizu et al., 2013),Cu_xAg_{1-x}/Al_2O_3 (Shimizu et al., 2011), Cu-HT (Dixit et al., 2013) and so on. From the above systems, although the precious metal-based catalysts present good catalytic activity, the scarcity and high cost greatly limited their commercial application. Consequently, the design and development of non-precious transition metal-based catalytic systems will be more meaningful. Among them, the Cu-containing catalyst systems show excellent catalytic activity, but there are few reports on the N-alkylation of amines with alcohols using Cu nanoparticle catalyst alone.

In recent years, the carbon materials-based catalysis systems have been received more research interest due to their good chemical and thermal stability, high specific surface area, porous structure, excellent electrical conductivity and controllable surface chemical properties (Serp and Figueiredo 2009, Zhang et al., 2020). Because heteroatoms differ from carbon atoms in their atomic size, electrical negativity, and bond length, introducing heteroatoms into porous carbon materials results in an uneven distribution of the charge of adjacent carbon atoms, which improves the electron transport performance of carbon materials while creating structural defects that contribute to improved catalytic performance (Shang and Gao 2019, Wang et al., 2022). In addition, heteroatoms, such as boron, nitrogen, fluorine, phosphorus, sulfur and so on, are used to modify the surface of carbon materials, which can effectively stabilize the loaded metal nanoparticles, improve the interaction between the metal and the carrier, enhance the catalytic activity, and broaden their potential applications (Gerber and Serp 2020, Das et al., 2023). Particularly, metal catalysis systems supported by heteroatoms-doped carbon materials have received extensive attention (Cao et al., 2017, Duan et al., 2018, Song et al., 2018, Yang et al., 2018, Gerber and Serp 2020). At present, carbon materials primarily come from fossil energies such as petroleum, coal, natural gas, etc, yet, they are becoming increasingly exhausted. Compared with fossil energies, biomass resources have many advantages including abundant reserves, biodegradability, low cost, and renewable, and can be used for the preparation of carbon materials.

In this work, the N,P-codoped porous carbon (NPC) was fabricated using P_2O_5 as the P source and wheat straw as the N and C sources, containing about 6 wt% of N from its proteins and amino acids. Further, the Cu nanoparticles were decorated on the fabricated N,P-codoped porous carbon (NPC) to construct a heterogeneous catalyst (Cu/NPC) for the reaction of N-alkylation of amines with alcohols. Importantly, the prepared Cu/NPC catalyst showed high yields for the synthesis of secondary amines from various aromatic amines and aromatic alcohols. To the best of our knowledge, there has been no report on the preparation and application of such Cu/NPC materials. Notably, the catalyst also exhibited high stability, environmental benignity and good reproducibility.

2. Experimental section

2.1. General information

All reagents were purchased from Energy Chemical or Tianjin Kemiou Chemical Reagent Co., Ltd. and used as received without further purification. The wheat straw was obtained from Yuzhong County, Gansu Province, China. The crystal structures of obtained catalysts were characterized by power X-ray diffraction (XRD, Rigaku D/max-2400 diffractometer using Cu-K α radiation), The XRD diffraction patterns were scanned in the 2θ range of 5-85° and the raw spectrum was provided. Nitrogen adsorption–desorption isotherms were measured at 77 K using Micromeritics ASAP 2460 analyzer. The pore-size distribution was calculated by Barrett, Joyner, and Halenda (BJH) method from the desorption isotherm. The morphology of catalysts was examined by field emission scanning electron microscopy (FE-SEM, SU8010,Hitachi Co.) with energy dispersive spectrometer (EDS). TEM analysis was carried out with a JEOL JEM-2100F field emission transmission electron microscope. The Cu loadings were measured by inductively coupled plasma mass spectrometry (ICP-MS, NexION350X,PerkinElmer). The X-ray photoelectron spectroscopy (XPS) measurements were performed with a Nexsa spectrometer (Thermo Fisher Inc.) and the data was processed using Avantage softwear. The Raman measurements were carried out with a Renishaw inVia Raman microscope at room temperature. The original spectra without any correction are provided and the intensity of G and D peaks used to calculate the I_D/I_G ratio.

2.2. Preparation of N, P-codoped porous carbon (NPC)

Firstly, the wheat straw was broken into pieces, ground into a powder with a grinder, passed through 100 mesh sieves, and dried. A certain amount of straw was homogeneously mixed with P_2O_5(quality ratio 1:3) in the hydrothermal reactor with teflon liner under an N_2 atmosphere at room temperature. After that, the mixture was kept at 160℃for 6 h (solvent-free solid phase reaction). Cooling to room temperature, the resultant black powder was then washed with deionized water until the pH of the filtrate was neutral. Finally, NPC was obtained after drying at 80℃for 6 h.

2.3. Preparation of the catalysts (Cu_n/NPC-x) [n is a number (such as 1, 2, 3.and so on) and × denotes the calcination temperature]

The Cu_n/NPC-x catalysts were prepared through the simple precipitation-deposition method. NPC(1 g) was dispersed in deionized water (100 mL) and $Cu(NO_3)_2{\cdot}3H_2O$ (0.38 g) was added to the solution under vigorous stirring. The pH value was adjusted to about 11 using NaOH solution (0.2 g/mL) and then the mixture was stirred for another 3.5 h at room temperature. The precipitating agent in this procedure is sodium hydroxide(NaOH), which allows the metal hydroxide species to be deposited on the carrier's surface.After that the

solid sample was filtered and washed with deionized water until the pH of the filtrate was neutral. The obtained solid was dried at 70℃ for 6 h, and then was put in a quartz boat and annealed at 450,550, and 650℃ for 2 h under in N_2 flow with a heating rate of 5 ℃/min. These catalysts were labeled Cu_2/ NPC-450, Cu_2/ NPC-550 and Cu_2/ NPC-550, and other catalysts (Cu_1/ NPC-550 and Cu_3/ NPC-550) were prepared following the same procedure.

2.4. Catalytic reaction

Amine(0.5 mmol), benzyl alcohol(1 mmol), catalyst(50 mg), KOH(30 mg) and cyclohexane (3 mL) were introduced into a glass reaction tube(35 mL). Argon was bubbled through the mixture for 5 min, then the tube was sealed with a Teflon lid. The reaction mixture was stirred at 140℃(oven temperature) for 12 h. After that, the reaction tube was cooled to room temperature and 10 mL ethyl acetate was added. Then the reaction mixture was analysed by GC–MS (Trace 1300-ISQ, Thermo) and GC-FID (Agilent 7890B). The crude reaction mixture was concentrated in vacuo and purified by column chromatography [ethyl acetate / petroleum ether (b.p. 60–90 ° C) = 1:20–1:50] to give the corresponding products.

3. Results and discussion

3.1. Catalyst characterization

As shown in Scheme 1, the N,P-codoped porous carbon (NPC) was prepared in a hydrothermal reactor using wheat straw and P_2O_5 as precursors without solvent. The P_2O_5 reacted with the hydroxide groups (–OH) in the biopolymer molecules of the biomass(e.g., cellulose or lignin) to form biopolymer phosphates, in the following process, the phosphates could dope P to the carbon matrix of the catalysts. In this process, P_2O_5 is not only provided as a P source but also as a dehydrating agent. The specific surface areas and pore size of the prepared catalysts were determined by N_2 adsorption–desorption measurements. The content of Cu was identified by inductively coupled plasma mass spectrometry (ICP-MS). The results were shown in Table 1. By comparison, the as-prepared NPC-550 catalyst presents the BET surface area and pore volume of 814 m^2 g^{-1} and 0.372 cm^3 g^{-1},which is much smaller than the as-fabricated Cu_n/NPC-550 samples. The NPC-550 catalyst showed a small BET surface area may be mainly due to the corrosion of alkali during the preparation process. As shown in Table 1, the BET surface area and pore volume of the Cu_n/NPC-550 decrease with increasing the Cu mass ratio. Moreover, the pore size of the samples increases slightly with the increase of Cu content. Nitrogen adsorption–desorption isotherms of the samples were also measured (Fig. S1a). The catalysts exhitied combined characteristics of type Ⅰand Ⅳ isotherms according to IUPAC classifications, indicating the catalysts contain hierarchically micro-, meso-, and macro-pores (Fig. S1b). On the basis of the ICP-MS analysis, the copper loading in Cu_1/NPC-550, Cu_2/NPC-550 and Cu_3/NPC-550 were 4.1 wt%, 8.1 wt% and 13 wt%, respectively. The surface chemical compositions of the catalysts were characterised by XPS, and the results are summarised in Table 2. The copper content on the surface of Cu_n/NPC-550 increase with the increase of copper loading amount. The NPC-550 catalyst showed a lower nitrogen content than Cu_n/NPC-550 owing to using copper(II) nitrate as raw material in the preparation process. In addition, the low phosphorus content in the Cu_n/NPC-550 is due to the use of alkali during metal loading, which destroys the structure of some biopolymer phosphates.

The crystalline structures of the samples were characterized by XRD. As shown in Fig. 1, the diffraction peak at about 23.0°, which is assigned to the (002) diffraction of the graphitic carbon(Dahbi et al., 2017), can be clearly visualized in the support(NPC-550). In contrast, Cu_n/NPC-550 samples show less intense reflection. Due to the use of NaOH during the loading of Cu, the layered structure of the carbon carrier is destroyed. For Cu_n/NPC-550 catalysts, the diffraction peaks at 2θ of 43.3°, 50.4°, 74.1° index to the (111), (200) and

Scheme 1 Schematic illustration for the synthetic procedure of the catalysts.

Table 1 BET surface area, pore volume, pore size and metal loadings of typical catalysts.

Catalysts	$S_{BET}(m^2g^{-1})$	Pore volume(cm^3g^{-1})	Pore size(nm)	Cu content (wt%)
NPC-550	814	0.372	3.49	–
Cu_1/NPC-550	1104.7	0.442	3.51	4.1
Cu_2/NPC-550	1063.4	0.438	3.62	8.1
Cu_3/NPC-550	966.6	0.411	3.85	13

Table 2 Chemical composition analysis of the catalysts from XPS.

Sample	Chemical composition(at%)		N	P	Cu
	C	O			
NPC-550	77.12	17.70	0.93	4.26	0
Cu_1/NPC-550	83.96	12.08	1.36	2.25	0.35
Cu_2/NPC-550	82.04	11.91	2.71	2.73	0.61
Cu_3/NPC-550	81.44	12.87	1.91	3.01	0.77

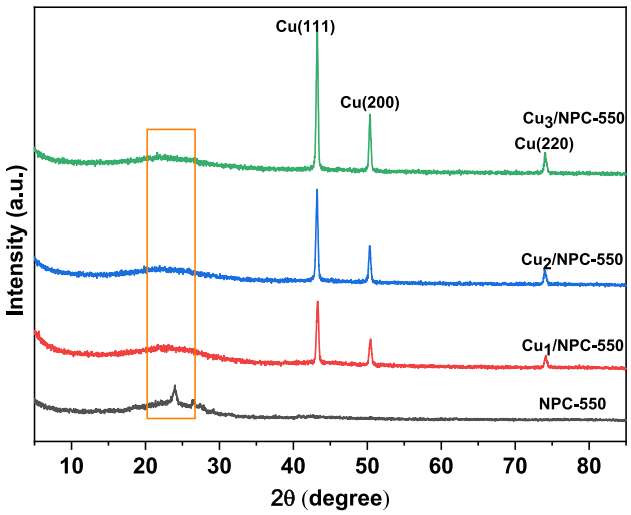

Fig. 1 XRD patterns of the fabricated catalysts.

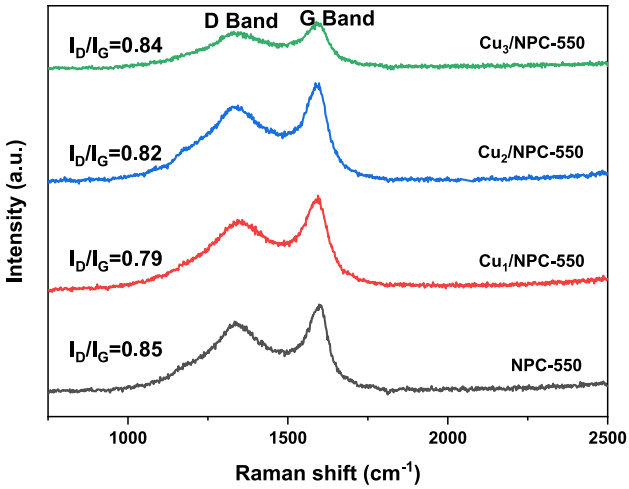

Fig. 2 Raman spectra of the fabricated catalysts.

(220) crystalline planes of metallic cubic copper (JCPDS No.04–0836), respectively(Wang et al., 2019), confirming the formation of Cu^0 during the calcination process. Noted that, with the increase of the Cu content, the diffraction peaks intensity of Cu gradually increases, which reveals the Cu ion was successfully loading on NPC. It also suggests that there are substantial interactions between copper ions and carbon carriers. The Raman spectroscopy of the fabricated catalysts is shown in Fig. 2. There are two peaks at around 1340 and 1590 cm^{-1}, corresponding to the D (defects and disorder) and G (sp2 graphitic carbon) bands of carbon, respectively. Generally, the intensity ratio between the D and G bands (I_D/I_G) indicates the degree of structural order with respect to graphitic structure(Ma et al., 2021). The I_D/I_G ratios of NPC-550, Cu_1/NPC-550, Cu_2/NPC-550, and Cu_3/NPC-550 were 0.85, 0.79, 0.82 and 0.84, respectively, implying that higher crystallization degree in all the samples and more defective sites or disorders in the NPC-550 (Bai et al., 2017). The lower the Cu content, the higher the crystallinity, indicating that the carbon layer is well crystallized when a small amount of Cu is present. Furthermore, the higher I_D/I_G values of catalysts with high metal loading than that of catalysts with low loading demonstrated that more defects and disorder were produced due to more Cu nanoparticles, which is consistent with the XRD results. It should be noted that, more defects can provide more catalytic active sites during the catalysis process.

To confirm the presence of Cu nanoparticles on the surface of the catalysts, the morphology of Cu_n/NPC-550 catalysts was determined by SEM and TEM as presented in Fig. 3 and Fig. 4, respectively. As shown in Fig. 3 (a), (c), and (e), the surface of supporter (NPC) is porous structure in favor of the dispersion of Cu particles. It is clearly observed that the majority of Cu particles were decorated on the surface of NPC in Fig. 3 (b), (d) and (f) which only differ in the number of copper particles. Moreover, the synthesized Cu particles ranged in size from 35 to 135 nm (Fig. 4a, inset and Fig. S2). Noted that, such Cu nanoparticles decorated on the

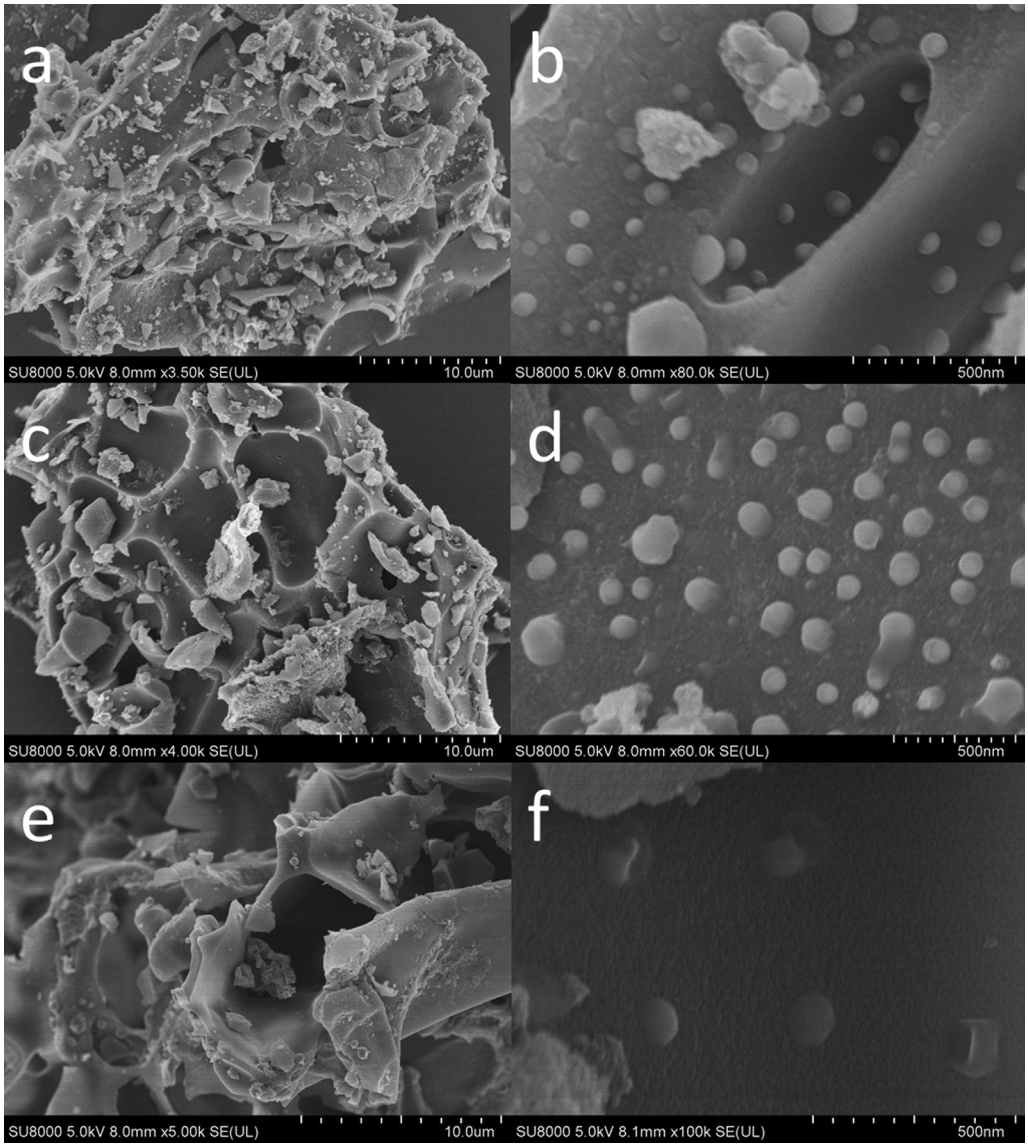

Fig. 3 SEM images of (a,b) Cu_3/NPC-550, (c,d) Cu_2/NPC-550, and (e,f) Cu_1/NPC-550.

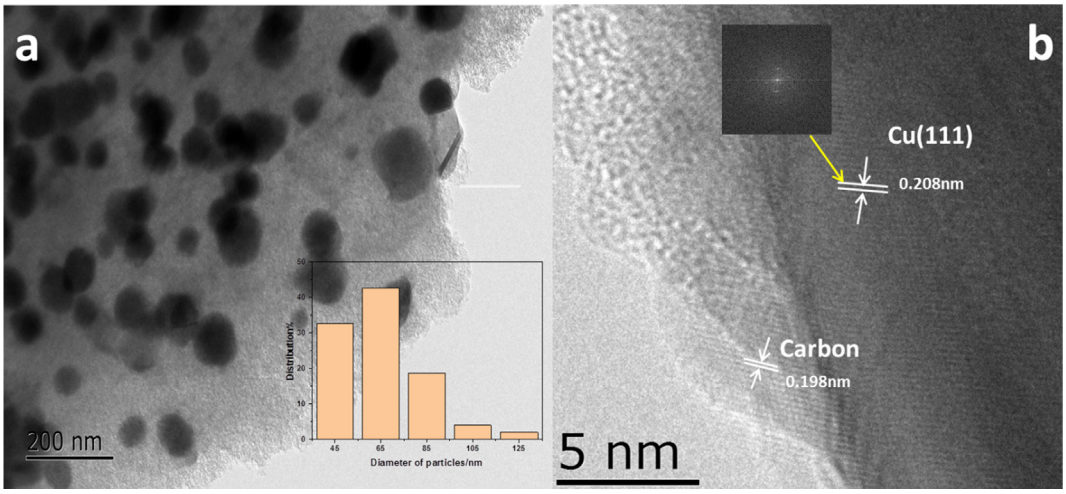

Fig. 4 (a) TEM image of the Cu_2/NPC-550, and (b) HRTEM image of the Cu_2/NPC-550.

surface of NPC can not only provide more surface active sites but also enhance the structural stability.

Fig. 4 (a) presents the TEM image of the Cu_2/NPC-550 catalysts, confirming the Cu nanoparticles were successfully decorated on NPC. The high-resolution TEM (HRTEM) image is displayed in Fig. 4b. As shown, the sample exhibits the lattice spacing value of 0.203 nm, corresponding to the (1 1 1) facet of metallic copper(Fan et al., 2018), which is in good agreement with the results of the XRD analysis as shown in Fig. 1. Moreover, other lattice fringes have a distance of 0.198 nm, which matches the carbon material in NPC. Further, EDS image mapping of the selected area was carried out to reveal the elemental distribution on the surface of the catalysts. As shown in Fig. 5 and Fig. S3, the elements of C, N, P and O are uniformly dispersed on the surface of the catalysts. By comparison, the catalyst possesses an uneven Cu distribution (Fig. 5f, Fig. S3f) owing to spherical Cu particles, which further validate the previous SEM and TEM results.

Further, XPS was performed to investigate the surface chemical composition of the catalysts. Fig. 6a shows the Cu 2p XPS profile for Cu_2/NPC-550. There are two peaks at 935.8 eV and 955.6 eV that can be attributed to the Cu $2p_{3/2}$ and Cu $2p_{1/2}$ binding energies, respectively. Moreover, the existence of satellite peaks (944.6 eV and 940.8 eV) indicates the oxidized copper Cu(II), owing to the surface of the catalysts in the air. Compared to the metallic Cu (932.6 eV), the Cu $2p_{3/2}$ binding energy of Cu_2/NPC-550 is positively shifted to ≈ 933.4 eV, implying that there is a strong interaction between the Cu particles and porous carbon framework (Wang et al., 2018). Noted that, the Cu 2p peaks can not be detected in the NPC-550 sample (Fig. S4a), which indicates that the sample surface does not contain Cu element. The Cu 2p XPS spectrum of Cu_3/NPC-550 is similar to that of Cu_2/NPC-550 with the same peak position and peak shape (Fig. S4b). Fig. 6b presents the N 1 s spectra of Cu_2/NPC-550. There are four types of N including oxidic-N (403.9 eV), graphitic-N (401.5 eV), pyrrolic N (400.1 eV), and pyridinic-N (398.9 eV)(Ma et al., 2021). In addition, similar results can be observed in NPC-550 and Cu_3/NPC-550 (Fig. S4c and S4d). The C1s spectra of the samples were deconvoluted into three peaks at 284.8, 285.4, and 287.3, which are attributed to graphitic sp^2 carbon (C–C), and carbon binding with phosphorus, and nitrogen or oxygen (C-P and C-N or C-O), respectively (Fig. 6 c, S4e and S4f) (Wang et al., 2018, Ma et al., 2020). The P 2p spectra (Fig. 6d, S4g and S4h) display three peaks at ≈133.2 eV, ≈134.0 eV and ≈135.0 eV corresponding to C-P, P-O and P = O(Wang et al., 2018), respectively. According to the above results of the spectra of C 1 s and P 2p, it can be confirmed that an additional P element is doped into the N-containing carbon network. Moreover, the XPS spectra of O 1 s for the samples also proved the existence of P-O, P = O and C-O/C = O (Fig. S5). Noted that, the differences in binding energy and intensity of P 2p peaks for all samples suggest that there may be some interaction between the P element and the Cu particles, and this interaction is also influenced by the metal content (Fig. 6d, S4g and S4h).

3.2. Catalyst performance

Following, we continued to investigate the catalytic activity of the samples for N-alkylation of amines with alcohols in cyclohexane. In this case, aniline and benzyl alcohol were chosen as model substrates. The corresponding results are compiled in Table 3. There are two main products of model reaction. One is N-benzylaniline, which is the target product, and the other is N-benzylideneaniline, which is a by-product. Firstly, NPC-550 was used as catalyst in the presence of KOH and the desired product was obtained in low yield (Entry 1). Furthermore, relatively lower yield of desired product was observed without KOH (Entry 2). Subsequently, when a small amount of Cu is loaded on the NPC-550 (Cu_1/NCP-550) as the catalyst, both the conversion of aniline and the selectivity of

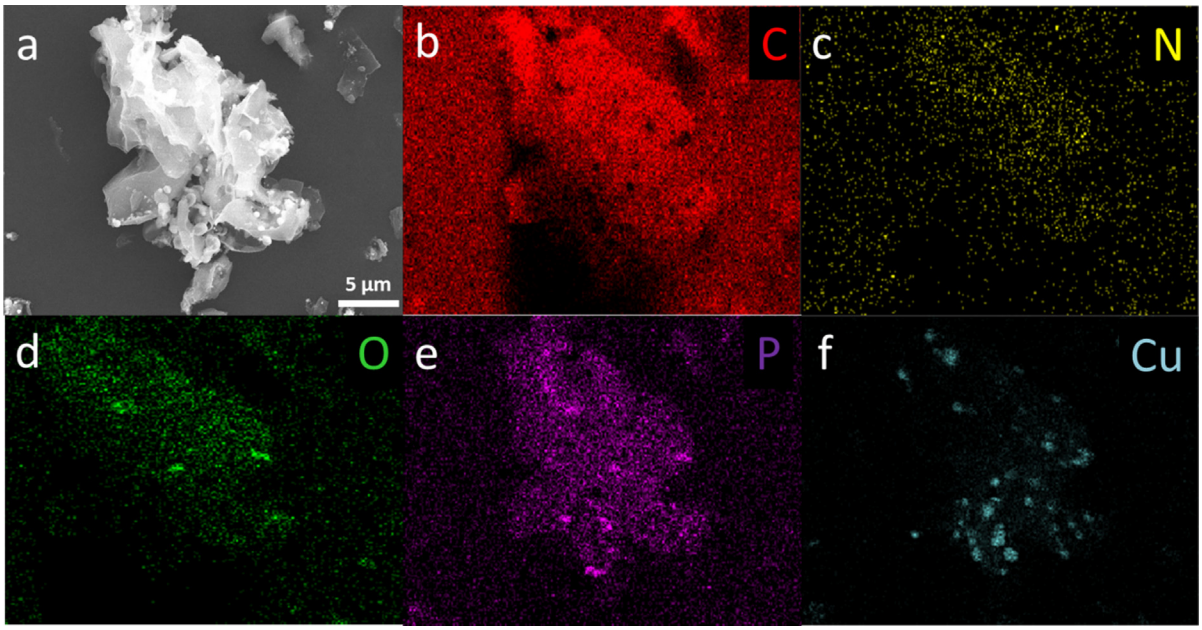

Fig. 5 (a-f) EDS mapping disclosing the elemental distribution of C, N, P, O and Cu on the surface of Cu_2/NPC-550.

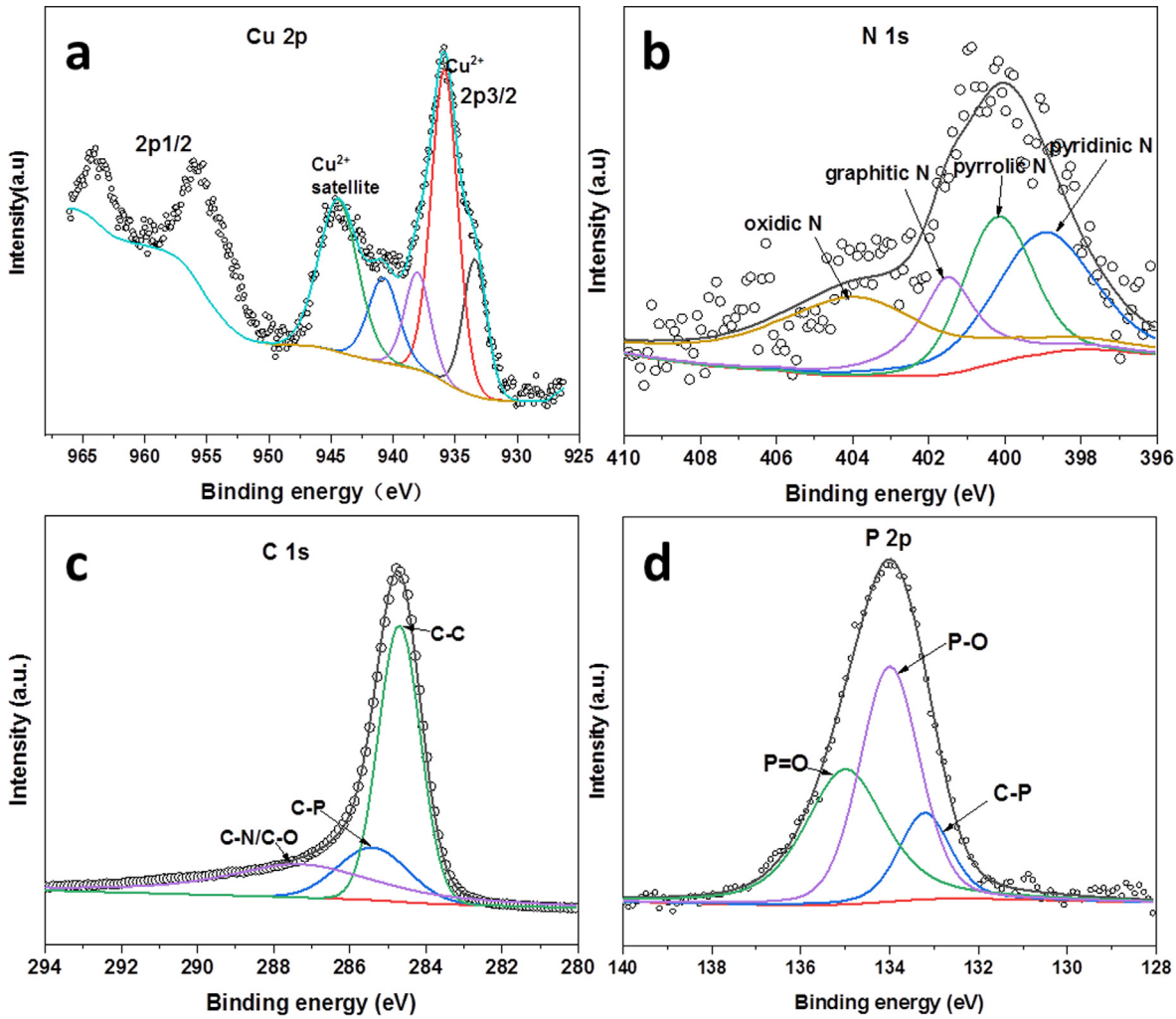

Fig. 6 XPS spectra of Cu_2/NPC-550, (a) Cu 2p, (b) N 1 s, (c) C 1 s, and (d) P 2p.

Table 3 Catalyst Screening and Reaction Condition Optimization[a.]

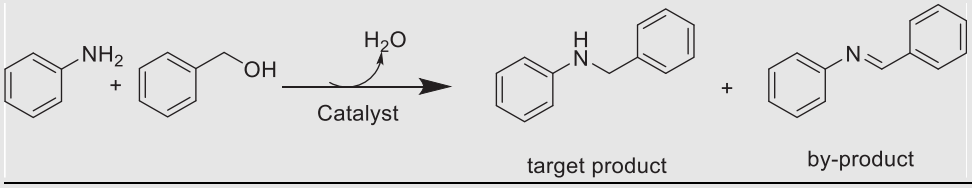

Entry	Catalyst	Conv.(%)[b]	Sel.(%)[b]
1	NPC-550	53	55
2	NPC-550[c]	15	32
3	Cu_1/NPC-550	96	85
4	Cu_2/NPC-550	100	95(87[d])
5	Cu_3/NPC-550	98	90
6	Cu_2/NPC-450	65	59
7	Cu_2/NPC-650	96	97
8	$Cu(NO_3)_2$	26	<1
9	KOH	25	68

a. Reaction conditions: aniline (0.5 mmol), benzyl alcohol(1 mmol), catalyst (50 mg), KOH (30 mg, AR,≥85%), cyclohexane (3 mL), Argon, 12 h, 140 °C. b. Conversion of aniline was determined by GC-FID without correction. c. without KOH d. Isolated yield.

Table 4 Substrate scope of functionalized aromatic amine with various benzylic alcohols[a.]

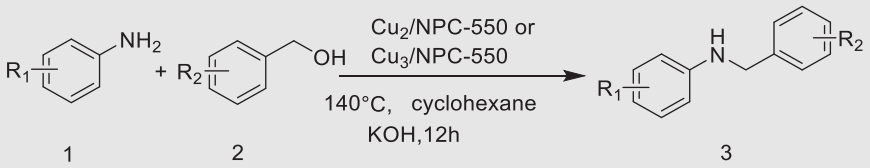

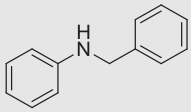
3a(87%)

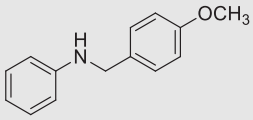

3b(85%)

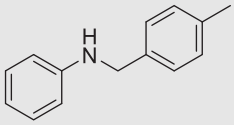
3c (86%)

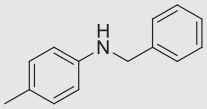
3d(79%)

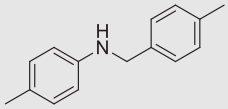
3e(91%)

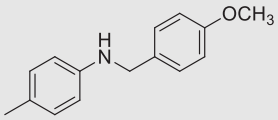

3f(89%)

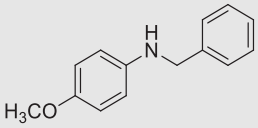

3g [b] (58%)

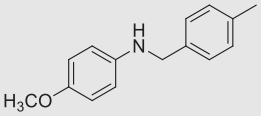

3h[b] (70%)

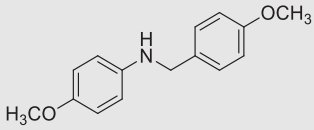

3i [b] (72%)

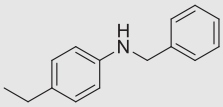
3j(85%)

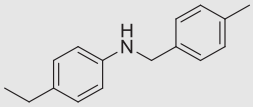
3k(81%)

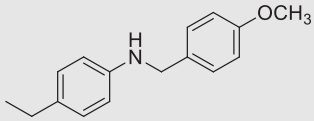

3l(80%)

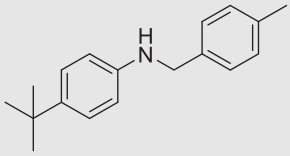
3m(91%)

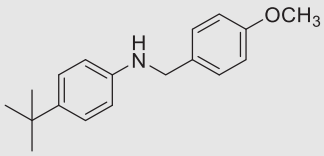

3n(80%)

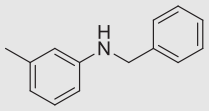
3o(85%)

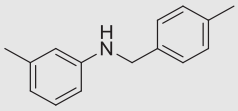
3p(86%)

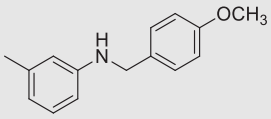

3q(66%) 3r(78%)

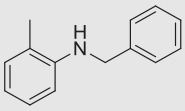

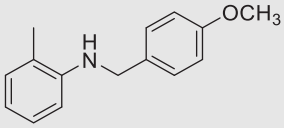

3s(70%)

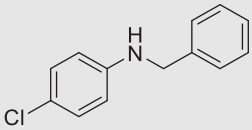

3t [b] (79%)

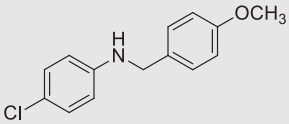

3u [b] (71%)

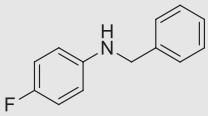

3v [b] (70%)

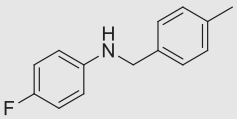

3w [b] (75%)

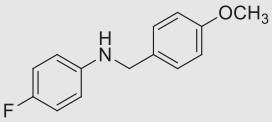

3x [b] (71%)

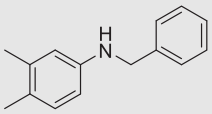
3y(80%)

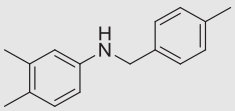
3z(90%)

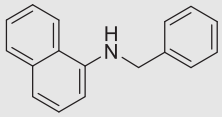
3aa(86%)

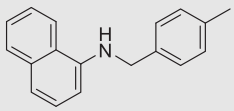
3ab(90%)

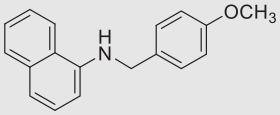

3ac(86%)

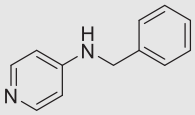

3ad(n.d)

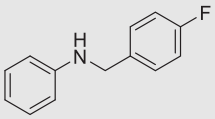

3ae(n.d)

a. Reaction conditions: amines (0.5 mmol), alcohol (1 mmol), Cu2/NPC-550 (50 mg), KOH (30 mg, AR, ≥85%), cyclohexane(3 mL), Argon, 12 h, 140℃.
b. The catalyst is Cu3/NPC-550 (50 mg), other conditions were same as "a".
c. Isolated yield. n.d = not detected.

desired product start to increase (Entry 3). In order to get a more effective catalyst, the Cu/NCP catalysts with different Cu loading and calcination temperature were screened and it was found that the Cu_2/NPC-550 was the most effective catalyst (Entries 4–7) and the catalytic efficiency of Cu_3/NPC-550 was also good (Entry 5). However, a considerably lower reactivity was observed in the presence of $Cu(NO_3)_2$ as catalyst or in absence of catalyst (Entries 8–9). From the results in Table 3, it can be seen that this catalytic system has excellent catalytic effect with the promotion of alkali additive.

Based on the optimized reaction condition, we turned to investigate the general applicability of the Cu nanocomposites catalyst in N-alkylation of structurally substituted aromatic amines and substituted aromatic alcohols. The results are shown in Table 4. It can be clearly seen that the isolated yields of N-alkylation reaction by aniline and aromatic alcohols without or with electron-donating groups were more than 85% (3a-3c). Anilines containing electron-donating (-Me, -Et, -t-Bu) groups were converted into their corresponding secondary amines in 66%-91% isolated yields (3d-3f, 3j-3q) with different aromatic alcohols. The o-methylaniline generally provided moderate yields owing to the effects of steric hindrance (3r and 3 s). Interestingly, the yields of desired products were lower under standard reaction conditions using the aniline with methoxy or halogen group as substrate, but when the catalyst was replaced with Cu_3/NPC-550 and other conditions remained unchanged, the moderate yield was obtained(3 g-3i, 3 t-3x). The result illustrates that the catalytic activity of our catalyst can be improved by adjusting the content of Cu for substrates with different substituents. To our delight, aromatic amines with slightly more complex including 3,4-dimethlaniline and naphthalen-2-amine could be activated and transformed to the corresponding secondary amines with excellent yields (3y-3ac). However, amines with stronger electron-withdrawing groups or aromatic alcohols with electron-withdrawing substituents failed to give the corresponding N-alkylation products under our reaction conditions (3ad-3ae).

Next, the recyclability of Cu_2/NPC-550 catalyst for the N-alkylation of aniline with benzyl alcohol was investigated.

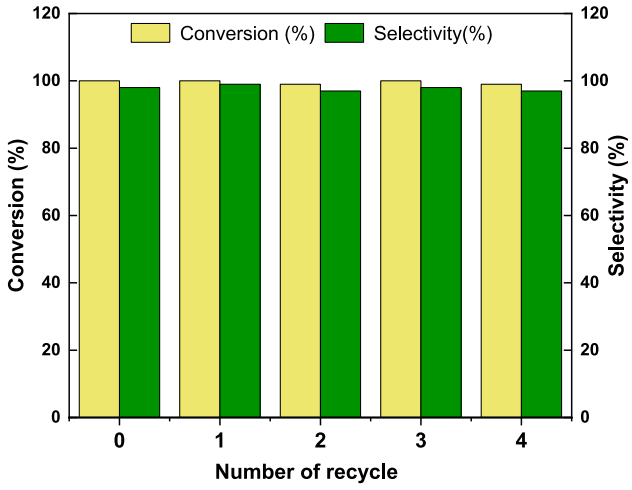

Fig. 7 The recycles ability of the catalyst (Reaction conditions: aniline (0.5 mmol), benzyl alcohol(1 mmol), Cu_2/NPC-550 (50 mg), KOH (30 mg, AR, ≥85%), cyclohexane (3 mL), Argon, 12 h, 140 °C. Conversion of aniline was determined byGC-FID without correction.).

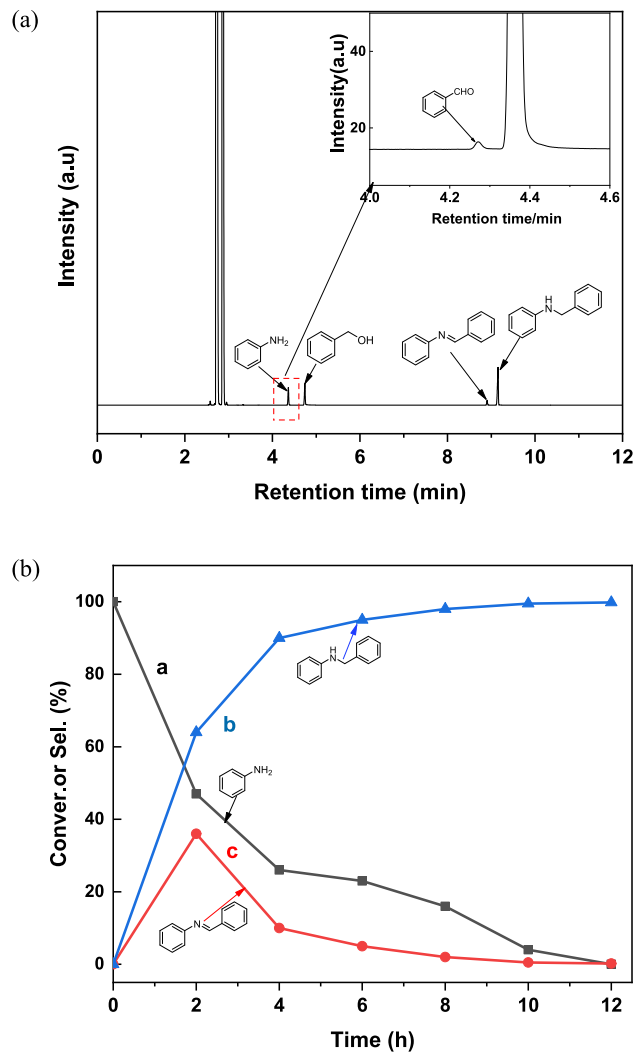

Fig. 8 (a) Gas chromatogram after 4 h of the reaction aniline with benzyl alcohol catalyzed by Cu_2/NPC.(b) Time-dependent variation of substrates and products during the reaction of aniline with benzyl alcohol catalyzed by Cu_2/NPC. Reaction conditions: aniline (0.5 mmol), benzyl alcohol(1 mmol), Cu_2/NPC-550 (50 mg), KOH (30 mg, AR,≥85%), cyclohexane(3 mL), Argon, 12 h, 140 °C. Conversion of aniline was determined byGC-FID without correction.

Upon completion of the reaction, the catalyst was easily recovered by filtration, washed with cyclohexane for several times and dried for the next run. As shown in Fig. 7, the catalyst can be successfully reused for five times without significant loss in the conversion and the selectivity, which manifests the excellent stability of the catalyst.

In order to examine the mechanism of the reaction, the N-alklation of aniline using benzyl alcohol were analyzed by GC and GC–MS. In particular, GC spectrum of the reaction mixture after 4 h is shown Fig. 8(a). There are four obvious peaks which correspond to aniline (retention time about 4.35 min), benzyl alcohol (retention time about 4.73 min), the intermediate imine N-benzylideneaniline product (retention time about 8.94 min) and the desired N-benzylaniline (retention time about 9.13 min) except for the solvent signals. A small amount of intermediate benzaldehyde which is quickly condensed with aniline to form the intermediate imine due to the presence of alkali, peak at about 4.26 min, can be observed (Fig. 8(a), inset). Although the peak is weak, it indicates that there is dehydrogenation process during the reaction. The time-dependent change in quantity variations of the substrate and products during the reaction is present in Fig. 8(b). These proved that the reaction has undergone a hydrogen transfer process which is consistent with the previously reported literature (Guillena et al., 2010, Irrgang and Kempe 2019).

On the basis of the above result, a plausible pathway can be proposed as shown in Fig. 9. As previously stated, The Cu-catalyzed N-alkylation reaction could preceed via the hydrogen-borrowing pathway. The benzyl alcohol is first actived and dehydrogenated over the Cu/NPC catalyst in the presence of base. Meanwhile, a Cu hydride specie (Cu-H) and benzaldehyde would be formed (Shimizu et al., 2011). Immediately, imine intermediate was generated by condensation of benzaldehyde and aniline. Finally, a hydrogen transfer from the Cu hydride species to the imine intermediate proceeds to yield a desired secondary amine. During the process of the reaction, the interconnection between the Cu nanoparticles and the surface of the supporter is enhanced (proved by XPS) due to the presence of N and P atoms. The result of the interaction is that Cu has a partial positive charge, which is conductive to the adsorption of reactants. As a base pro-

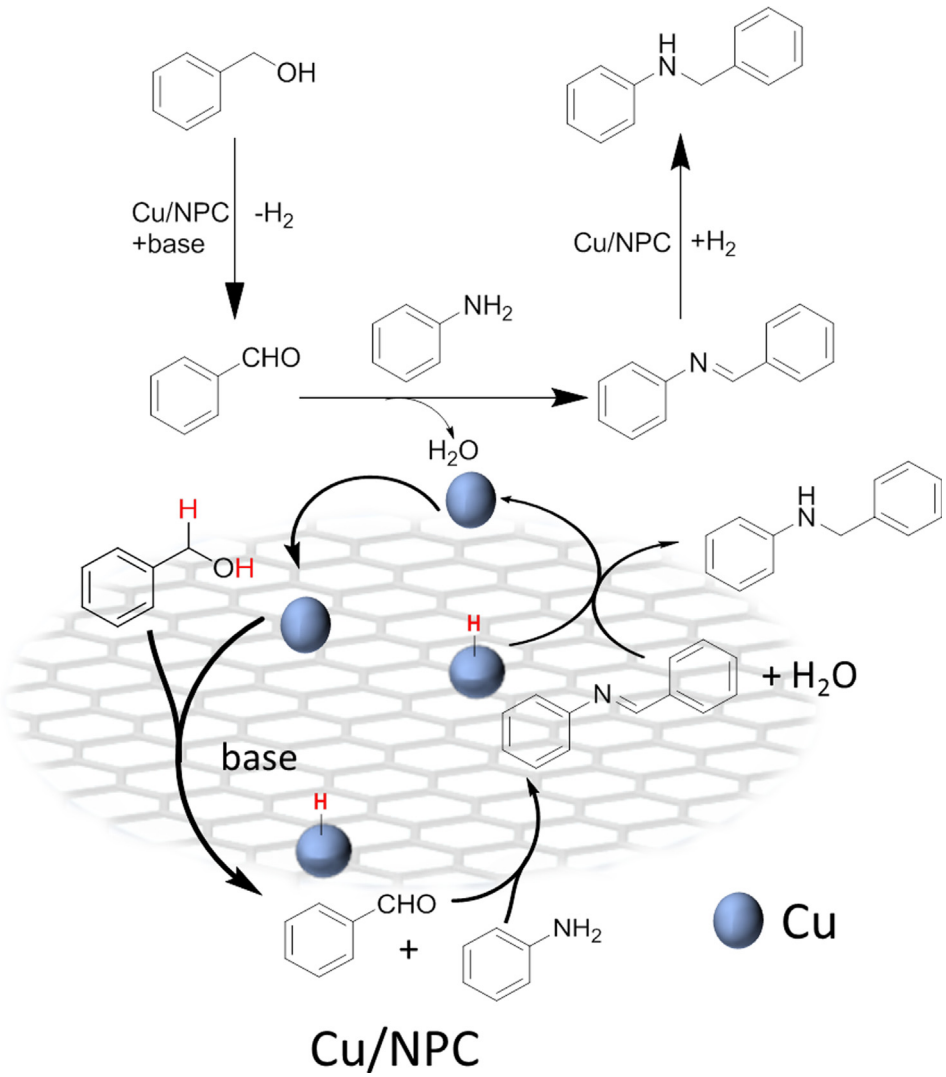

Fig. 9 Proposed mechanism for the reaction of aniline and benzyl alcohol over Cu/NPC.

moter, the addition of KOH increased the activity and selectivity to target product(Liu et al., 2012).

4. Conclusion

In summary, low cost and easily prepared heterogeneous Cu/NPC catalysts have been shown efficient catalytic performance for N-monoalkylation of aromatic amines with aromatic alcohols. The advantages of the catalysts system are given as follows: (1) the preparation of carbon material uses biomass as a precursor, which is low-cost, readily available, and renewable. (2) The biomass-derived carbon has a large surface area, high pore volume, and porous structure, which is beneficial for the dispersion of Cu particles and offers more active sites for the reaction. (3) The doping of N and P heteroatoms can not only show synergistic catalytic performance but also improve the structural stability of the catalyst. So that there is no significant loss in both activity and selectivity after at least 4 reuses. Our results provide an effective strategy for other organic transformations via a green and facile way. Initial mechanistic investigations confirm that this is a hydrogen-autotransfer process, but the particular involvement of N,P atoms is not well understood, More research is being conducted to increase catalytic performance, investigate reaction mechanisms, and broaden the range of applications for our catalyst

CRediT authorship contribution statement

Dong Zhang: . **Jingjing Tian:** . **Yunyun Yan:** Formal analysis. **Lina Zhang:** Conceptualization, Formal analysis, Investigation, Writing – original draft. **Hongyu Hu:** Formal analysis, Validation, Writing – review & editing.

Declaration of Competing Interest

The authors declare that they have no known competing financial interests or personal relationships that could have appeared to influence the work reported in this paper.

Acknowledgements

The authors thank Dr Le Wang, Dr Jian Xiao for GC-MS, LC-MS and NMR measurements, respectively. This work was supported by the Baoji University of Arts and Sciences (ZK16059), Research Foundation of Education Department of Shaanxi Province (18JS009) and partially supported by the Zhejiang basic public welfare fund (No.LGF22H300015).

Appendix A. Supplementary material

Supplementary data to this article can be found online at https://doi.org/10.1016/j.arabjc.2023.105124.

References

Alshammari, A.S., Natte, K., Kalevaru, N.V., et al, 2020. Scalable preparation of stable and reusable silica supported palladium nanoparticles as catalysts for N-alkylation of amines with alcohols. J. Catal. 382, 141–149. https://doi.org/10.1016/j.jcat.2019.12.012.

Bai, Y., Fang, L., Xu, H., et al, 2017. Strengthened synergistic effect of metallic MxPy (M = Co, Ni, and Cu) and carbon layer via peapod-like architecture for both hydrogen and oxygen evolution reactions. Small 13, 1603718. https://doi.org/10.1002/smll.201603718.

Balamurugan, G., Ramesh, R., Malecki, J.G., 2020. Nickel(II)–NΛNΛO pincer type complex-catalyzed N-alkylation of amines with alcohols via the hydrogen autotransfer reaction. J. Org. Chem. 85, 7125–7135. https://doi.org/10.1021/acs.joc.0c00530.

Cao, Y., Mao, S., Li, M., et al, 2017. Metal/porous carbon composites for heterogeneous catalysis: Old catalysts with improved performance promoted by N-doping. ACS Catal. 7, 8090–8112. https://doi.org/10.1021/acscatal.7b02335.

Carey, J.S., Laffan, D., Thomson, C., et al, 2006. Analysis of the reactions used for the preparation of drug candidate molecules. Org. Biomol. Chem. 4, 2337–2347. https://doi.org/10.1039/B602413K.

Chang, Y.J., Chow, T.J., 2009. Triaryl linked donor acceptor dyads for high-performance dye-sensitized solar cells. Tetrahedron 65, 9626–9632. https://doi.org/10.1016/j.tet.2009.09.036.

Chung, H., Chung, Y.K., 2018. Cobalt-rhodium heterobimetallic nanoparticle-catalyzed N-alkylation of amines with alcohols to secondary and tertiary amines. J Org Chem. 83, 8533–8542. https://doi.org/10.1021/acs.joc.8b01109.

Corma, A., Ródenas, T., Sabater, M.J., 2010. A Bifunctional Pd/MgO solid catalyst for the one-pot selective N-monoalkylation of amines with alcohols. Chem. – Eur. J. 16, 254–260. https://doi.org/10.1002/chem.200901501.

Cui, X., Zhang, Y., Shi, F., et al, 2011. Organic ligand-free alkylation of amines, carboxamides, sulfonamides, and ketones by using alcohols catalyzed by heterogeneous Ag/Mo oxides. Chem. A Eur. J. 17, 1021–1028. https://doi.org/10.1002/chem.201001915.

Dahbi, M., Kiso, M., Kubota, K., et al, 2017. Synthesis of hard carbon from argan shells for Na-ion batteries. J. Mater. Chem. A 5, 9917–9928. https://doi.org/10.1039/C7TA01394A.

Das, A., Mondal, S., Hansda, K.M., et al, 2023. A critical review on the role of carbon supports of metal catalysts for selective catalytic hydrogenation of chloronitrobenzenes. Appl. Catal. A 649,. https://doi.org/10.1016/j.apcata.2022.118955 118955.

Dixit, M., Mishra, M., Joshi, P.A., et al, 2013. Clean borrowing hydrogen methodology using hydrotalcite supported copper catalyst. Catal. Commun. 33, 80–83. https://doi.org/10.1016/j.catcom.2012.12.027.

Duan, Y., Song, T., Dong, X., et al, 2018. Enhanced catalytic performance of cobalt nanoparticles coated with a N, P-codoped carbon shell derived from biomass for transfer hydrogenation of functionalized nitroarenes. Green Chem. 20, 2821–2828. https://doi.org/10.1039/C8GC00619A.

Emayavaramban, B., Chakraborty, P., Manoury, E., et al, 2019. Cp*Co(iii)-catalyzed N-alkylation of amines with secondary alcohols. Org. Chem. Front. 6, 852–857. https://doi.org/10.1039/C8QO01389F.

Fan, R., Chen, C., Han, M., et al, 2018. Highly dispersed copper nanoparticles supported on activated carbon as an efficient catalyst for selective reduction of vanillin. Small 14, 1801953. https://doi.org/10.1002/smll.201801953.

Feng, X., Huang, M., 2021. Effect of the ancillary ligand in N-heterocyclic carbene iridium(III) catalyzed N-alkylation of amines with alcohols. Polyhedron 205,. https://doi.org/10.1016/j.poly.2021.115289 115289.

Fertig, R., Irrgang, T., Freitag, F., et al, 2018. Manganese-catalyzed and base-switchable synthesis of amines or imines via borrowing hydrogen or dehydrogenative condensation. ACS Catal. 8, 8525–8530. https://doi.org/10.1021/acscatal.8b02530.

Froidevaux, V., Negrell, C., Caillol, S., et al, 2016. Biobased amines: From synthesis to polymers; present and future. Chem. Rev. 116, 14181–14224. https://doi.org/10.1021/acs.chemrev.6b00486.

Furukawa, S., Suzuki, R., Komatsu, T., 2016. Selective activation of alcohols in the presence of reactive amines over intermetallic PdZn: Efficient catalysis for alcohol-based N-alkylation of various amines. ACS Catal. 6, 5946–5953. https://doi.org/10.1021/acscatal.6b01677.

Gerber, I.C., Serp, P., 2020. A theory/experience description of support effects in carbon-supported catalysts. Chem. Rev. 120, 1250–1349. https://doi.org/10.1021/acs.chemrev.9b00209.

Guillena, G., Ramón, D.J., Yus, M., 2010. Hydrogen autotransfer in the N-alkylation of amines and related compounds using alcohols and amines as electrophiles. Chem. Rev. 110, 1611–1641. https://doi.org/10.1021/cr9002159.

Hayes, K.S., 2001. Industrial processes for manufacturing amines. Appl. Catal. A: General 221, 187–195. https://doi.org/10.1016/S0926-860X(01)00813-4.

He, L., Lou, X.-B., Ni, J., et al, 2010. Efficient and clean gold-catalyzed one-pot selective N-alkylation of amines with alcohols. Chem. – Eur. J. 16, 13965–13969. https://doi.org/10.1002/chem.201001848.

Huang, M., Li, Y., Liu, J., et al, 2019. A bifunctional strategy for N-heterocyclic carbene-stabilized iridium complex-catalyzed N-alkylation of amines with alcohols in aqueous media. Green Chem. 21, 219–224. https://doi.org/10.1039/c8gc02298d.

Huang, M., Li, Y., Lan, X.-B., et al, 2021. Ruthenium(ii) complexes with N-heterocyclic carbene–phosphine ligands for the N-alkylation of amines with alcohols. Org. Biomol. Chem. 19, 3451–3461. https://doi.org/10.1039/D1OB00362C.

Irrgang, T., Kempe, R., 2019. 3d-metal catalyzed N- and C-alkylation reactions via borrowing hydrogen or hydrogen autotransfer. Chem Rev. 119, 2524–2549. https://doi.org/10.1021/acs.chemrev.8b00306.

Jiménez, M.V., Fernández-Tornos, J., González-Lainez, M., et al, 2018. Mechanistic studies on the N-alkylation of amines with alcohols catalysed by iridium(i) complexes with functionalised N-heterocyclic carbene ligands. Cat. Sci. Technol. 8, 2381–2393. https://doi.org/10.1039/C7CY02488F.

Kallmeier, F., Fertig, R., Irrgang, T., et al, 2020. Chromium-catalyzed alkylation of amines by alcohols. Angew. Chem. Int. Ed. 59, 11789–11793. https://doi.org/10.1002/anie.202001704.

Karaca, E.Ö., Dehimat, Z.I., Yaşar, S., et al, 2021. Ru(II)-NHC catalysed N-Alkylation of amines with alcohols under solvent-free conditions. Inorg. Chim. Acta 520,. https://doi.org/10.1016/j.ica.2021.120294 120294.

Lengvinaite, S., Grazulevicius, J.V., Grigalevicius, S., et al, 2008. Cross-linkable aromatic amines as materials for insoluble hole-transporting layers in light-emitting devices. Synth. Met. 158, 213–218. https://doi.org/10.1016/j.synthmet.2008.01.004.

Li, C., Wan, K.F., Guo, F.Y., et al, 2019. Iridium-catalyzed alkylation of amine and nitrobenzene with alcohol to tertiary amine under base- and solvent-free conditions. J. Org. Chem. 84, 2158–2168. https://doi.org/10.1021/acs.joc.8b03137.

Liu, H., Chuah, G.-K., Jaenicke, S., 2012. N-alkylation of amines with alcohols over alumina-entrapped Ag catalysts using the "borrowing hydrogen" methodology. J. Catal. 292, 130–137. https://doi.org/10.1016/j.jcat.2012.05.007.

Liu, X., Hermange, P., Ruiz, J., et al, 2016. Pd/C as an efficient and reusable catalyst for the selective N-alkylation of amines with alcohols. ChemCatChem. 8, 1043–1045. https://doi.org/10.1002/cctc.201501346.

Luo, N., Zhong, Y., Wen, H., et al, 2020. Cyclometalated iridium complex-catalyzed N-alkylation of amines with alcohols via borrowing hydrogen in aqueous media. ACS Omega 5, 27723–27732. https://doi.org/10.1021/acsomega.0c04192.

Ma, L.-L., Liu, W.-J., Hu, X., et al, 2020. Ionothermal carbonization of biomass to construct sp2/sp3 carbon interface in N-doped biochar as efficient oxygen reduction electrocatalysts. Chem. Eng. J. 400,. https://doi.org/10.1016/j.cej.2020.125969 125969.

Ma, L.-L., Hu, X., Liu, W.-J., et al, 2021. Constructing N, P-dually doped biochar materials from biomass wastes for high-performance bifunctional oxygen electrocatalysts. Chemosphere 278,. https://doi.org/10.1016/j.chemosphere.2021.130508 130508.

Mandi, U., Kundu, S.K., Salam, N., et al, 2016. Ag@polypyrrole: A highly efficient nanocatalyst for the N-alkylation of amines using alcohols. J Colloid Interface Sci. 467, 291–299. https://doi.org/10.1016/j.jcis.2016.01.017.

Martínez-Asencio, A., Ramón, D.J., Yus, M., 2011. N-Alkylation of poor nucleophilic amines and derivatives with alcohols by a hydrogen autotransfer process catalyzed by copper(II) acetate: scope and mechanistic considerations. Tetrahedron 67, 3140–3149. https://doi.org/10.1016/j.tet.2011.02.075.

Minakawa, M., Okubo, M., Kawatsura, M., 2015. Selective direct N-alkylation of amines with alcohols using Iron(III) phthalocyanine chloride under solvent-free conditions. Bull. Chem. Soc. Jpn. 88, 1680–1682. https://doi.org/10.1246/bcsj.20150217.

Paul, P., Bhanja, P., Salam, N., et al, 2017. Silver nanoparticles supported over mesoporous alumina as an efficient nanocatalyst for N-alkylation of hetero (aromatic) amines and aromatic amines using alcohols as alkylating agent. J. Colloid Interface Sci. 493, 206–217. https://doi.org/10.1016/j.jcis.2016.12.072.

Prabha, D., Pachisia, S., Gupta, R., 2021. Cobalt mediated N-alkylation of amines by alcohols: role of hydrogen bonding pocket. Inorg. Chem. Front. 8, 1599–1609. https://doi.org/10.1039/D0QI01374A.

Rosler, S., Ertl, M., Irrgang, T., et al, 2015. Cobalt-catalyzed alkylation of aromatic amines by alcohols. Angew. Chem. Int. Ed. Engl. 54, 15046–15050. https://doi.org/10.1002/anie.201507955.

Serp, P. and J. L. s. Figueiredo, 2009. Carbon materials for catalysis.

Shang, S.S., Gao, S., 2019. Heteroatom-enhanced metal-free catalytic performance of carbocatalysts for organic transformations. ChemCatChem. 11, 3730–3744. https://doi.org/10.1002/cctc.201900336.

Shimizu, K.-I., Shimura, K., Nishimura, M., et al, 2011. Silver cluster-promoted heterogeneous copper catalyst for N-alkylation of amines with alcohols. RSC Adv. 1, 1310–1317. https://doi.org/10.1039/C1RA00560J.

Shimizu, K.-I., Kon, K., Onodera, W., et al, 2013. Heterogeneous Ni catalyst for direct synthesis of primary amines from alcohols and ammonia. ACS Catal. 3, 112–117. https://doi.org/10.1021/cs3007473.

Song, T., Ren, P., Duan, Y., et al, 2018. Cobalt nanocomposites on N-doped hierarchical porous carbon for highly selective formation of anilines and imines from nitroarenes. Green Chem. 20, 4629–4637. https://doi.org/10.1039/C8GC01374H.

Veefkind, V.A., Lercher, J.A., 1998. Zeolite catalysts for the selective synthesis of mono- and diethylamines. J. Catal. 180, 258–269. https://doi.org/10.1006/jcat.1998.2275.

Vellakkaran, M., Singh, K., Banerjee, D., 2017. An efficient and selective nickel-catalyzed direct N-alkylation of anilines with alcohols. ACS Catal. 7, 8152–8158. https://doi.org/10.1021/acscatal.7b02817.

Wang, R., Dong, X.-Y., Du, J., et al, 2018. MOF-derived bifunctional Cu3P nanoparticles coated by a N, P-codoped carbon shell for hydrogen evolution and oxygen reduction. Adv. Mater. 30, 1703711. https://doi.org/10.1002/adma.201703711.

Wang, K., Gao, W., Jiang, P., et al, 2019. Bi-functional catalyst of porous N-doped carbon with bimetallic FeCu for solvent-free resultant imines and hydrogenation of nitroarenes. Mol. Catal. 465, 43–53. https://doi.org/10.1016/j.mcat.2018.12.029.

Wang, Y.-Z., Tang, Z.-H., Shen, S.-L., et al, 2022. The influence of heteroatom doping on the performance of carbon-based electrocatalysts for oxygen evolution reactions. New Carbon Mater. 37, 321–336. https://doi.org/10.1016/S1872-5805(22)60591-2.

Wei, D., Yang, P., Yu, C., et al, 2021. N-alkylation of amines with alcohols catalyzed by Manganese(II) chloride or Bromopentacarbonylmanganese(I). J. Org. Chem. 86, 2254–2263. https://doi.org/10.1021/acs.joc.0c02407.

Wong, C.M., Peterson, M.B., Pernik, I., et al, 2017. Highly efficient Rh (I) homo- and heterogeneous catalysts for C-N couplings via hydrogen borrowing. Inorg. Chem. 56, 14682–14687. https://doi.org/10.1021/acs.inorgchem.7b02586.

Wu, P.-Y., Lu, G.-P., Cai, C., 2021. Synthesis of an Fe–Pd bimetallic catalyst for N-alkylation of amines with alcohols via a hydrogen auto-transfer methodology. Green Chem. 23, 396–404. https://doi.org/10.1039/D0GC03725G.

Yang, S., Zhu, Y., Cao, C., et al, 2018. Controllable synthesis of multiheteroatoms co-doped hierarchical porous carbon spheres as an ideal catalysis platform. ACS Appl. Mater. Interfaces 10, 19664–19672. https://doi.org/10.1021/acsami.8b03283.

Zhang, L.-H., Shi, Y., Wang, Y., et al, 2020. Nanocarbon catalysts: recent understanding regarding the active sites. Adv. Sci. 7, 1902126. https://doi.org/10.1002/advs.201902126.

Zhang, M., Wu, S., Bian, L., et al, 2019. One-pot synthesis of Pd-promoted Ce–Ni mixed oxides as efficient catalysts for imine production from the direct N-alkylation of amine with alcohol. Cat. Sci. Technol. 9, 286–301. https://doi.org/10.1039/c8cy01857j.